ANNALS OF GEOPHYSICS, 69, 2026; doi:10.4401/ag-9408
OPEN ACCESS

Tectonic evolution of the Central Anatolian Crystalline Complex: Insights from using magnetic and gravity data

Gülten Aktaş*,[1]

(1) Gümüşhane University, Department of Geophysical Engineering, Gümüşhane, Turkey

Article history: received August 14, 2025; accepted February 16, 2026

Abstract

This study investigates the inherited crustal architecture and concealed tectonic boundaries of the Kırşehir Massif, a key component of the Central Anatolian Crystalline Complex (CACC), using satellite-derived potential field datasets. Earth Magnetic Anomaly Grid 2 (EMAG2) magnetic anomalies and World Gravity Map 2012 (WGM2012) Bouguer gravity data were analyzed together with multiple edge-detection filters, including Total Horizontal Gradient (THG), Tilt Angle (TA), Theta Map (TM), and Tilt Angle of Horizontal Derivative Amplitude (TAHG), to enhance structural boundaries and identify subsurface discontinuities prior to geological interpretation. The enhanced magnetic and gravity fields reveal two principal lineament sets trending NW-SE and NE-SW, which coincide with major lithological contacts, fault zones, and the boundaries of the İzmir-Ankara-Erzincan Suture Zone (IAESZ) and Inner Tauride Suture Zone (ITSZ). Quantitative lineament classification based on azimuth and length statistics further confirms three dominant structural orientations (NW-SE, NE-SW, and E-W), reflecting both inherited suture-related structures and younger transtensional deformation. By integrating filtered anomaly gradients with regional geological constraints, this study provides the most detailed potential-field-based structural model of the Kırşehir Block to date and offers new insights into crustal inheritance, lithospheric segmentation, and the multi-phase tectonic evolution of Central Anatolia.

Keywords: Central Anatolian Crystalline Complex; Edge detection; WGM2012; EMAG2; Kırşehir Massif

1. Introduction

The tectonics of Anatolia is the result of the combination of various tectonic events and entities from the Paleozoic to the present (Ketin, 1966; Okay, 1989; Okay et al., 1994; Robertson et al., 2012, 2013; Şengör and Yılmaz, 1981; Yılmaz et al., 1995). The geodynamic evolution of Tethys has made the most important contribution to the geological diversity of Turkey today. The main elements of Anatolian tectonics are the suture zones formed by the closure of ocean basins. The remnants of Neotethys are structurally characterized by ophiolites, metamorphic basements, and ophiolitic melanges in decreasing order (Parlak et al., 2009). Tethys ocean remnants are observed in the İzmir-Ankara-Erzincan suture zone (IAESZ) between the Pontides and the Anatolide-Tauride Platform and the Kırşehir Block (KB) (Okay and

Tüysüz, 1999). The Central Anatolian region is a large, triangular area defined by its structure. It is bounded by the Central Anatolian Fault Zone to the east, the Akşehir Fault Zone to the west, the IAESZ to the north, and the Inner Tauride suture zone (ITSZ) to the south (Temiz et al., 2009). The KB, one of the main tectonic units of Turkey, borders this area. The KB generally consists of ophiolites placed on high-grade metamorphic rocks. The metamorphic, igneous, and ophiolitic rock assemblages in Central Anatolia are known as the Central Anatolian Crystalline Complex (CACC) (Göncüoğlu et al., 1991, 1993). Although the area bounded by the IAESZ in the north and the ITSZ in the south has been divided into various zones, forming the KB, the exact boundaries of this area are still the subject of debate. The study area covers a wide area of Central Anatolia, where the borders of these Pontide-Kırşehir and Tauride blocks, IAESZ, and the still controversial ITSZ are drawn (Fig. 1). There is no consensus in the literature on the location and continuity of the KB and ITSZ boundaries (Whitney and Dilek, 1998). Understanding the tectonic relationship by determining the boundaries of these two suture zones constitutes the main purpose of this study. Evaluation of magnetic and gravity anomalies together with geological and geophysical constraints provides a basic scientific framework for seismic hazard analysis and disaster risk reduction studies by enabling a more comprehensive and

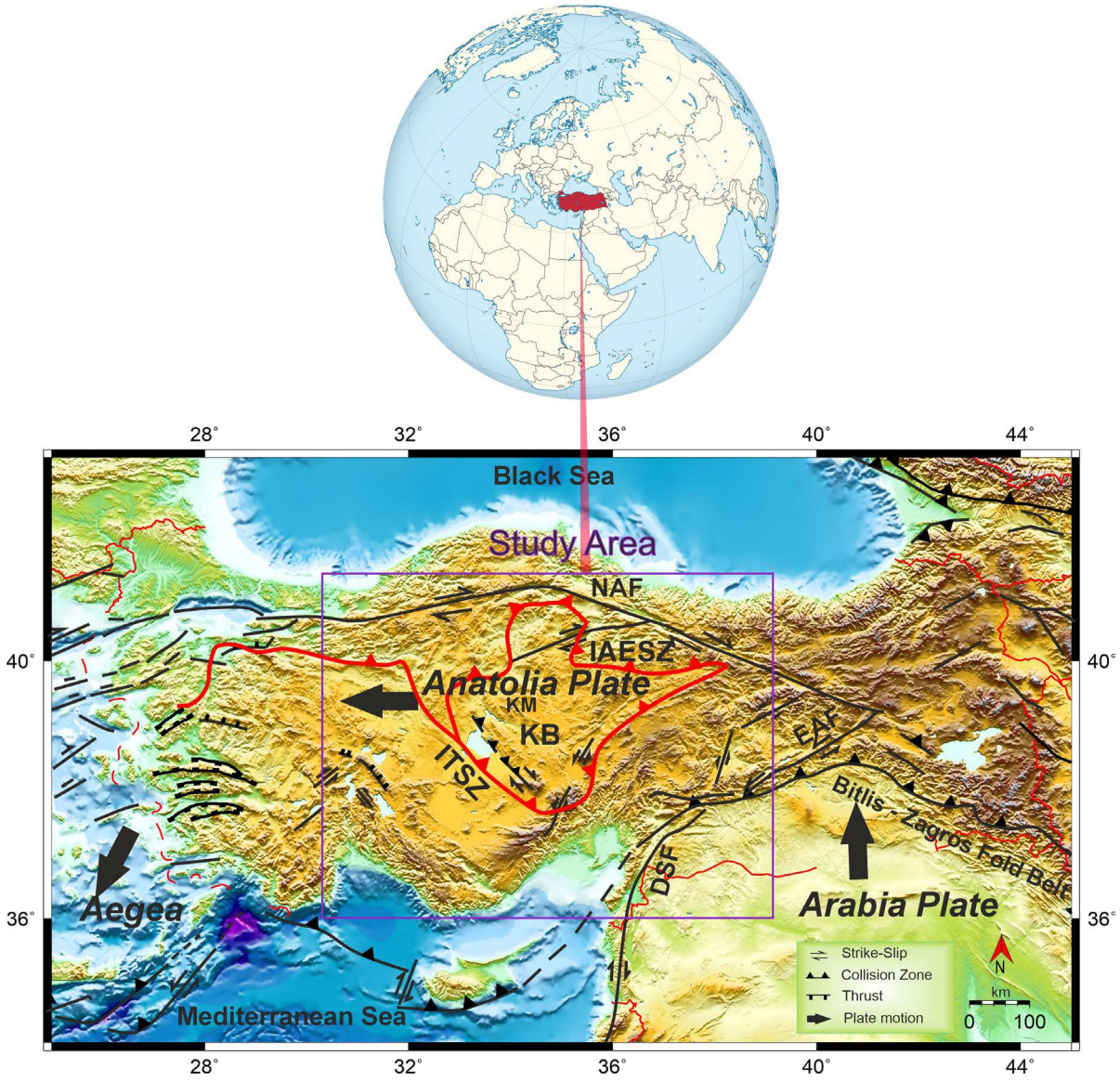

Figure 1. Tectonic map of Turkey and the surrounding areas (Modified from Şaroğlu et al., 1992; Bozkurt, 2001; Taymaz et al., 2007; and Emre et al., 2013). Abbreviations: EAF: East Anatolian Fault, NAF: North Anatolian Fault, DSF: Dead Sea Fault, KM: Kırşehir Massif, KB: Kırşehir Block, IAESZ: İzmir-Ankara-Erzincan Suture Zone, ITSZ: Inner Tauride Suture Zone. The base map was created using General Mapping Tools (GMT) (Wessel et al., 2013). The study area is shown with a purple square.

reliable analysis of underground faulting mechanisms. Despite numerous studies on the tectonic framework of the CACC and the KB (Fig. 1), there remains a lack of high-resolution geophysical constraints on the precise boundaries and structural relationships of the IAESZ and the ITSZ. Magnetic and gravity anomalies are among the basic geophysical tools in determining the basin architecture, fault geometries and structural evolution of sedimentary fill, thanks to their capacity to visualize subsurface density and magnetization contrasts (Hinze et al., 2013).

Magnetic and gravity methods are two fundamental potential field techniques that provide complementary information in identifying geological structures extending from shallow to deep by measuring varying magnetization and density contrasts across the crust. The magnetic method is particularly sensitive to the distribution of magnetizable rocks and enables the identification of both shallow and intermediate igneous and tectonic units within a depth range of approximately 0-20 km. Shallow anomalies are generally associated with dykes, fault zones, volcanic veins, and near-surface intrusives, while longer-wavelength anomalies reflect deeply buried igneous bodies and magnetic basement topography. The gravity method, on the other hand, has the capacity to resolve a broad depth spectrum, from shallow to the Moho level, due to density differences. At shallow levels (0-1 km), changes in overburden thickness, fault slips, and near-surface density anomalies can be distinguished, while at intermediate depths (1-10 km), basin geometry, graben/horst structures, and voluminous igneous-sedimentary bodies can be reliably modeled. Gravity anomalies dominated by broader wavelength components reveal crustal thickness variations, continental block boundaries, and Moho topography at depths ranging from 10-40 km. The integrated evaluation of both methods allows for the unraveling of relationships between shallow tectonic elements and deep crustal architecture, providing significant contributions to a more reliable multi-scale interpretation of magmatic evolution, basin development, and the regional tectonic framework.

Gravity and magnetic methods play a crucial role in imaging deep-seated faults and crustal-scale structural features, and they are particularly valuable in regions where key tectonic boundaries remain obscured. Central Anatolia represents one such area, where the structural configuration of the Kırşehir Massif and its relationship to surrounding suture zones are still subjects of debate. Despite numerous geological studies, the extent to which inherited crustal fabrics influence the present-day tectonic architecture of this region remains insufficiently constrained. In this context, the present study aims to evaluate how large-scale gravity and magnetic anomaly patterns can be used to clarify the crustal structure and tectonic boundaries of the Kırşehir Massif and, more broadly, to shed light on the geodynamic evolution of Central Anatolia. By focusing on the regional signatures of major lithospheric elements, the study seeks to determine whether potential field data can meaningfully resolve long-lived structural domains and contribute to ongoing discussions regarding the role of crustal inheritance in shaping Anatolia's current tectonic framework. These goals provide the broader geodynamic motivation of the research and establish its relevance within the wider context of Neotethyan orogenic processes. This study fills this gap by combining satellite-based Earth Magnetic Anomaly Grid 2 (EMAG2) magnetic data and World Gravity Map 2012 (WGM2012) gravity data with advanced edge detection techniques and provides new insights into the geodynamic framework of Central Anatolia.

This study provides a new high-resolution structural framework for the Kırşehir Block and surrounding suture zones by integrating EMAG2 magnetic anomalies and WGM2012 Bouguer gravity data with multiple edge-detection filters. Unlike previous works, including the recent regional-scale study of Özsöz and Toker (2025), our analysis resolves the geometry, continuity, and segmentation of the IAESZ and ITSZ at a finer spatial scale. The combined interpretation of directional derivatives, filtered anomaly gradients, and lineament trend classification offers new evidence for the crustal architecture and concealed tectonic boundaries of Central Anatolia. These results represent the most detailed potential-field-based structural model published for this region to date.

2. Geology of the study area

Ophiolites represent fragments of oceanic lithosphere that become emplaced onto continental or oceanic crust during major tectonic processes such as subduction, obduction, and continental collision (Bodinier and Godard, 2005; Coleman, 1977). Globally, they form key components of convergent margin systems and offer critical insights into the geodynamic evolution of ancient ocean basins. Many ophiolite complexes around the world record spreading processes that occurred in supra-subduction zone environments, reflecting the complex interplay between plate convergence, slab rollback, and back-arc extension (Yılmaz et al., 1993).

Central Anatolia preserves several of these oceanic fragments within the CACC, where metamorphic, igneous, and ophiolitic units are juxtaposed (Göncüoğlu et al., 1991, 1993; Pourteau et al., 2010; van Hinsbergen et al., 2016).

The ophiolites in this region occur as isolated blocks dispersed between major suture zones. Within the study area, ophiolites marking the IAESZ dominate the northern margin of the CACC, whereas Central Anatolian ophiolites appear as discontinuous slices further inland. The primary geological elements relevant to this study include the Central Anatolian ophiolites, the Kırşehir Massif, the Niğde Massif, and the intervening sedimentary basins (Fig. 2). The Niğde Massif comprises high-grade metamorphic rocks forming the southern structural high of the CACC.

The metamorphic units in Western and Central Anatolia are classified into three main massifs according to their metamorphic grades and structural settings: the Kırşehir Block in the northeast, the Tavşanlı Zone in the northwest, and the Afyon Zone, which borders both zones to the south (Figs. 1, 2). The Kırşehir Block, located in the central part of Anatolia, exhibits a triangular massif character, also known as the CACC (Göncüoğlu et al., 1991; Lefebvre, 2011). The Tavşanlı Zone, first described by Okay (1984), is an approximately east-west-striking, ~300 km long and ~50 km wide belt composed of rocks metamorphosed under high-pressure-low-temperature conditions. This zone contains metasedimentary units of continental origin belonging to the northern margin of the Anatolide-Tauride continent and is believed to have undergone metamorphism during the Cretaceous period when the Tavşanlı rocks were subducted beneath the oceanic lithosphere (van Hinsbergen et al., 2016). The Afyon Zone forms an approximately 800 km-long belt surrounding the western, southern, and eastern parts of the Kırşehir Block (van Hinsbergen et al., 2016).

The study area lies between two major Neotethyan suture zones: the IAESZ to the north and the ITSZ to the south. The IAESZ represents the closure of the northern branch of the Neotethys Ocean through northward subduction during the Late Cretaceous-Late Paleocene and the subsequent collision between the Sakarya Zone and the Kırşehir Block (Şengör and Yılmaz, 1981; Görür et al., 1984; Yılmaz et al., 1997; Okay and Tüysüz, 1999). The Kırşehir Block is largely composed of ophiolitic, metamorphic, and granitic units emplaced during this convergence history. Further south, the ITSZ records the final stages of Neotethyan closure and contributes to the complex internal architecture of the CACC. Regionally, the Tuz Lake and Central Anatolian fault systems follow and exploit these major suture zones, further modifying the crustal structure.

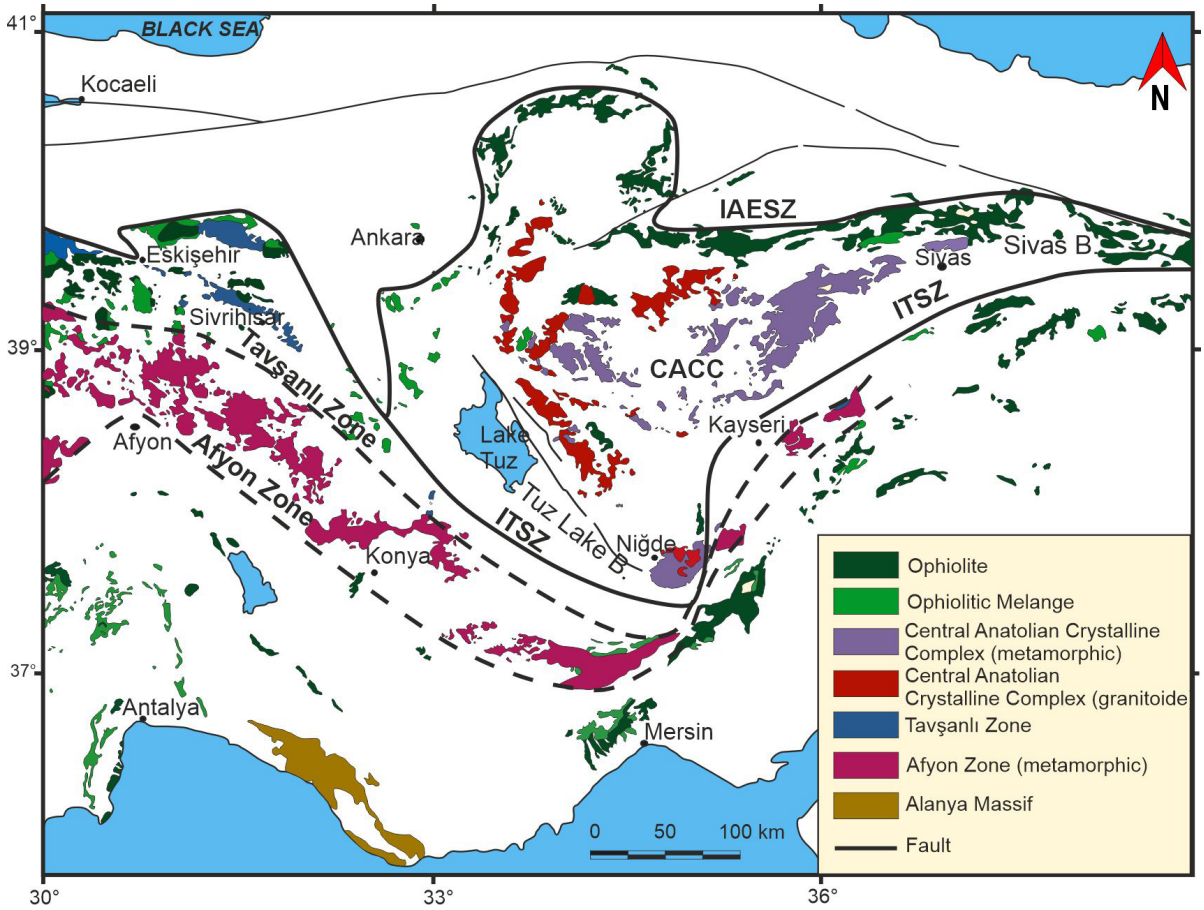

Figure 2. Geological map of the study area (Modified after MTA, 2002; van Hinsbergen et al., 2016; Pourteau et al., 2010; Çörtük et al., 2024).

3. Materials and methods

The magnetic dataset used in this study is the EMAG2 global grid, compiled from satellite, airborne, and marine magnetic surveys at a resolution of 2 arc minutes (~4 km). EMAG2 represents the current international standard for regional-scale magnetic anomaly interpretation and predominantly reflects long-wavelength crustal magnetic variations. Although highly suitable for identifying large-scale structural trends, its resolution limits the imaging of shallow or small-scale geological features. The gravity dataset used in this work, WGM2012, is a 1-arc-minute (~2 km) global Bouguer gravity model constructed from terrestrial, marine, and satellite gravimetric measurements. WGM2012 includes topographic and isostatic corrections and is designed to capture regional Bouguer anomaly patterns. Due to the global processing of both datasets, short-wavelength lithological or near-surface variations may be smoothed, an important factor that has been carefully considered throughout the interpretation. Because EMAG2 and WGM2012 are globally processed, homogenized, and upward-continued datasets, they inherently represent long-wavelength (regional) magnetic and gravity fields. EMAG2 suppresses short-wavelength signals during its compilation to better highlight broad crustal trends (Maus et al., 2009; Hemant and Maus, 2005), while WGM2012 integrates fully corrected gravimetric data to provide a uniform regional Bouguer field (Balmino et al., 2012; Bonvalot et al., 2012). Therefore, applying an additional regional-residual separation to these datasets would be physically inappropriate and may introduce artificial distortions. In accordance with international practice, both datasets were used directly for regional tectonic interpretation. To enhance shorter-wavelength structural elements, multiple edge-detection filters (THG, TA, TM, TAHG) were applied, effectively fulfilling the functional role of residual analysis.

3.1 Reduce to the pole (RTP)

At mid- and low magnetic latitudes, anomalies generated by symmetrically shaped source bodies typically appear asymmetric because the inducing geomagnetic field has a non-vertical inclination and non-zero declination. This causes displacement, skewness, and amplitude distortion in magnetic anomalies, shifting anomaly peaks away from the true location of their sources (Blakely, 1995; Nabighian et al., 2005). Such asymmetric behaviour complicates geological interpretation by obscuring the lateral boundaries and geometric characteristics of subsurface structures. The RTP transformation compensates for these effects by re-projecting the observed magnetic field to the theoretical condition of a vertically oriented inducing field (Baranov, 1957; Baranov and Naudy, 1964). RTP removes the directional dependence of magnetization, producing symmetric, centered anomalies whose maxima are located directly above their causative bodies. If the magnetization were entirely vertical, RTP transformed anomalies would form radially symmetric, bell-shaped patterns that closely reflect the true geometry and spatial extent of the sources.

3.2 Edge detection techniques

3.2.1 Total horizontal gradient (THG)

The Total Horizontal Gradient (THG) is a fundamental edge-detection operator used in the interpretation of potential-field data, particularly magnetic and gravity anomalies. The THG method enhances short- to intermediate-wavelength components while attenuating long-wavelength regional trends, making it particularly effective for imaging shallow to moderately deep subsurface structures. As a horizontal edge-detection technique, THG generates amplitude maxima directly above the lateral boundaries of the causative sources, thereby facilitating the delineation of sharp structural discontinuities. Although the method does not fully normalize the amplitude differences between shallow and deep-seated anomalies, it offers the advantage of being comparatively less sensitive to noise, thus providing stable and reliable boundary detection in potential-field datasets (Pham et al., 2018; Pham et al., 2020). The THG is calculated as the square root of the sum of the squared horizontal derivatives, thereby quantifying the lateral rate of change of the field. The THG is expressed as follows (Cordell and Grauch, 1985):

$$THG = \sqrt{\left(\frac{\partial F}{\partial x}\right)^2 + \left(\frac{\partial F}{\partial y}\right)^2} \quad (1)$$

where, $\partial F/\partial x$ and $\partial F/\partial y$ are the x and y derivatives of the potential field data, F, respectively.

3.2.2 Tilt angle (TA)

The Tilt Angle (TA) is defined as the arctangent of the ratio between the vertical derivative and the total horizontal derivative of the magnetic field. This attribute effectively emphasizes major magnetic lineaments, enhances the recognition of source boundaries, and supports depth estimation of the causative bodies (Miller and Singh, 1994; Verduzco et al., 2004; Salem et al., 2008). The TA values range between $-\pi/2$ and $\pi/2$ radians. In this representation, positive amplitudes typically occur directly above magnetic sources, negative amplitudes appear outside the source regions, and values close to zero delineate the edges of the magnetic bodies (Miller and Singh, 1994). The formulation of TA is as follows:

$$TA = \tan^{-1} \frac{\frac{\partial F}{\partial z}}{\sqrt{\left(\frac{\partial F}{\partial x}\right)^2 + \left(\frac{\partial F}{\partial y}\right)^2}} \tag{2}$$

3.2.3 Theta map (TM)

The Theta map (TM), as formulated by Wijns et al. (2005), combines the horizontal gradient magnitude with the analytic signal amplitude to enhance lateral discontinuities in potential-field data. The transformation is defined mathematically as:

$$TM = a\cos \frac{\sqrt{\left(\frac{\partial F}{\partial x}\right)^2 + \left(\frac{\partial F}{\partial y}\right)^2}}{|AS|} \tag{3}$$

In this method, the analytic signal $|AS|$ is defined as the square root of the sum of the squared horizontal and vertical derivatives, providing a measure of the total gradient of the field. This transformation produces elevated values over the main source regions, while minima occur along the boundaries of magnetic or gravity bodies, thus effectively delineating lateral heterogeneities. Owing to these characteristics, the Theta map is particularly useful for outlining sharp lithological contacts, fault zones, and intrusive margins.

3.2.4 Tilt angle of the horizontal gradient (TAHG)

The Tilt Angle of the Horizontal Gradient (TAHG) is an edge-enhancement technique derived from the combination of the horizontal gradient magnitude and the tilt angle transformation. Ferreira et al. (2013) proposed the TAHG, a modified form of the TA (Miller and Singh, 1994), to map the source edges and balance the amplitudes of shallow and deep source anomalies. The TAHG filter is defined as;

$$TAHG = \operatorname{atan} \frac{\frac{\partial THG}{\partial z}}{\sqrt{\left(\frac{\partial THG}{\partial x}\right)^2 + \left(\frac{\partial THG}{\partial y}\right)^2}} \tag{4}$$

where $\partial THG/\partial x$, $\partial THG/\partial y$ and $\partial THG/\partial z$ are the derivatives of the horizontal gradient of the field F in the x,y,z directions respectively. The maximum TAHG values represent the boundaries of geological structures. Compared with other methods, this method is more effective at identifying the boundaries of deep geological bodies.

4. Results

4.1 EMAG2

This study uses EMAG2 magnetic data (Maus et al., 2009; Meyer et al., 2017), which is a compilation of measurements collected from satellites, the sea, and the air. The EMAG2 data have an approximate resolution of 2 arc minutes.

The magnetic anomaly grid is provided at an altitude of approximately 4 km above sea level (Maus et al., 2009). While EMAG2 provides a consistent regional coverage, its resolution may smooth short-wavelength anomalies, potentially limiting the detection of small-scale geological features. The total magnetic anomaly is shown in Fig. 3. In order to overcome the dipole phenomenon of magnetic data, it is RTP, as shown in Fig. 4. In the RTP magnetic anomaly map of the study area, magnetic values vary between –601 and 783 nT.

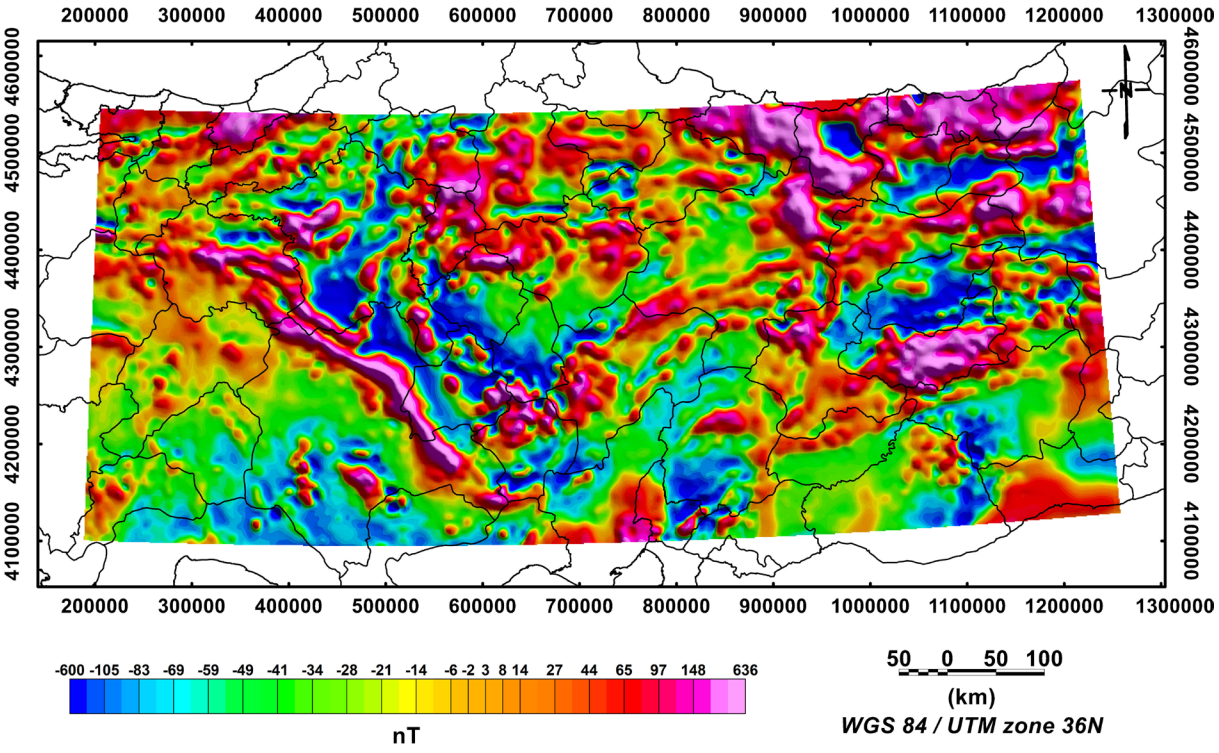

Figure 3. Total magnetic anomaly map (Black continuous lines on the map indicate the city boundaries of the study area).

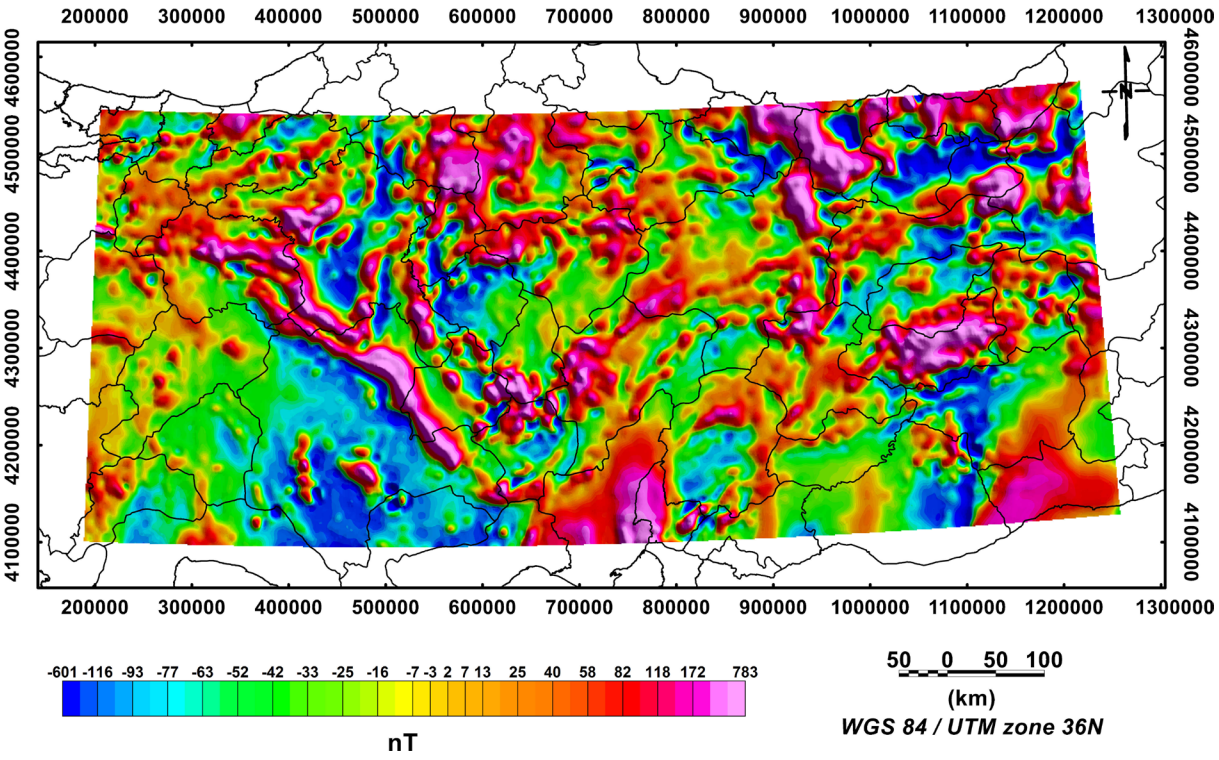

Figure 4. RTP magnetic anomaly map (Black continuous lines on the map indicate the city boundaries of the study area).

4.1.1 Application of edge detection techniques to magnetic data

In order to provide a more interpretable map in terms of causative bodies, RTP was applied to the magnetic data of the study area (Fig. 4). Figures 5 and 6a, b, c show the results of applying different edge detection filters (THG, TA, TM, TAHG) to the RTP data. The THG was applied to the RTP magnetic anomaly data of the study area to determine the edges of the magnetic structures and is shown in Fig. 5. The large area characterized by high magnetic anomaly values (−0.207 to 0.132 nT/km) exhibits a structural boundary similar to the V-shaped central part of the study area (Fig. 5). The peaks, which are closed near the edge, are linear and merge into an oval at the bottom and are arranged in the NW-SE, NE-SW directions. These orientations are well defined by the maximum points of the horizontal derivatives, and these maximum points generally follow the boundaries of the anomalies on the TA map.

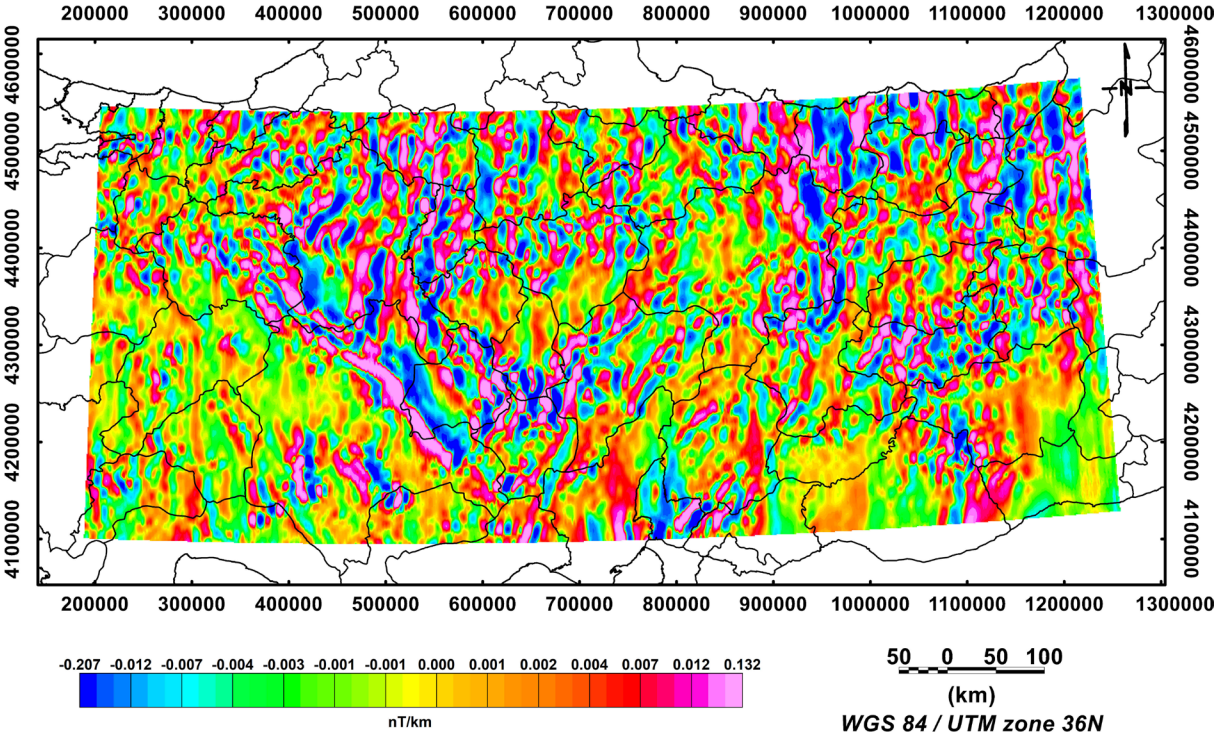

Figure 5. THG map of RTP data (Black continuous lines on the map indicate the city boundaries of the study area).

The TA filter is applied to magnetic and gravity data in the detection and mapping of shallow basement geological structures. In this study, the TA filter was applied to the RTP anomaly data to provide better resolution of geological structural features and to determine the boundaries of these geological structures. In Fig. 6a, the TA map applied to the RTP anomaly data is negative when above the magnetic source bodies and positive when outside the magnetic source bodies. The zero contours on the TA map indicate the location of the sharp transitions, with these zero contours also representing the limits of the structure. The major structural elements in the TA and THG anomaly maps show a very good correlation between the peaks of the THG and the zero contour lines of the TA. The results of the TM and TAHG analyses are presented in Figs. 6b and 6c, respectively. The TM application highlighted regional-scale structural discontinuities within the magnetic field, enabling the general boundary geometry of the source geological units to be revealed. However, the TM map only highlights a few major structures with distinct magnetic contrasts, thus providing limited resolution of the details of shallow, low-amplitude anomalies. The TAHG results, on the other hand, exhibited higher edge sensitivity compared to TM, contributing to a sharper, more continuous, and more distinct mapping of structural boundaries. Therefore, while TM is useful for identifying general trends and the regional magnetic framework, TAHG is particularly effective in identifying sharp structural transitions and potential fault boundaries.

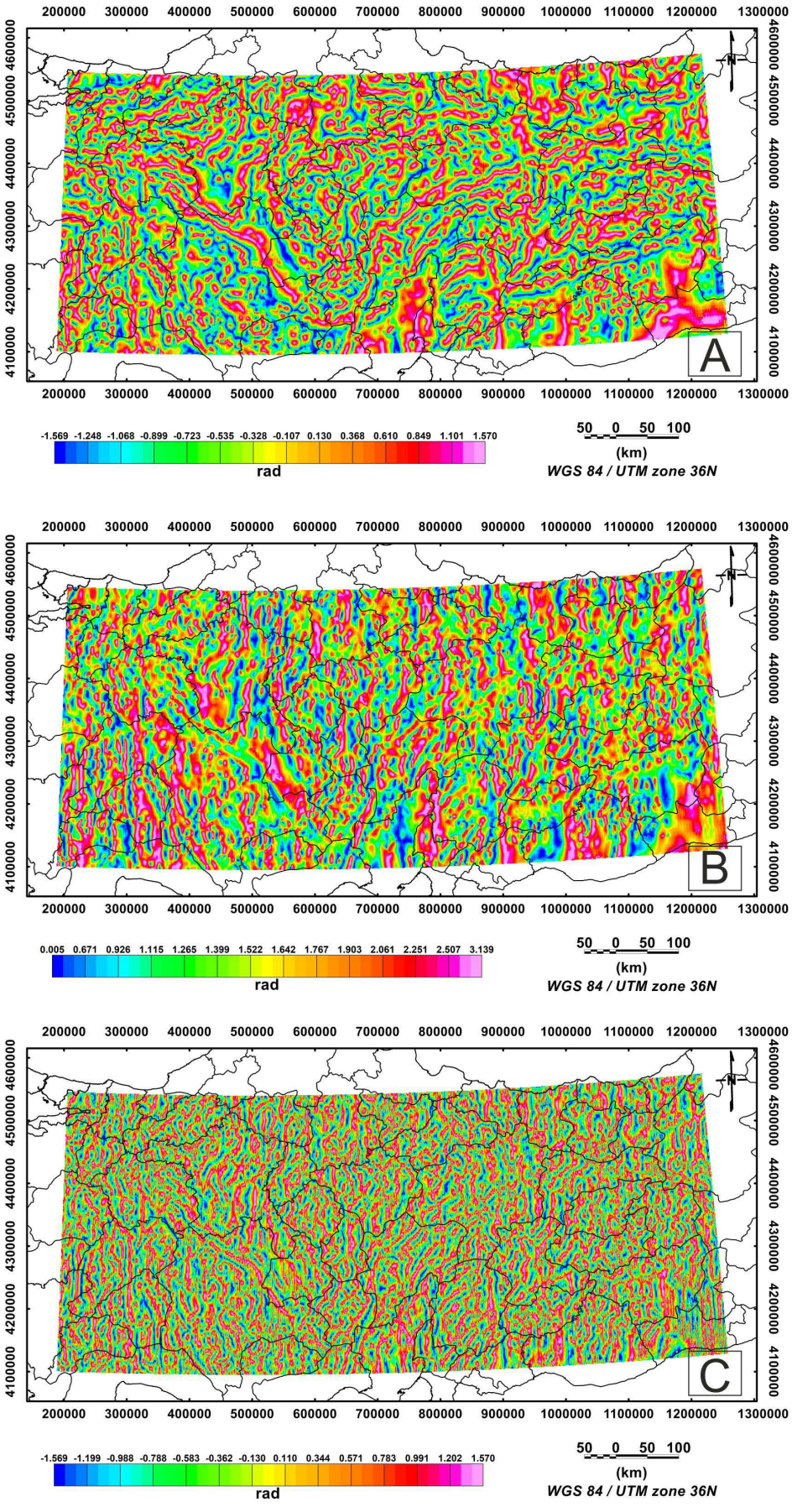

Figure 6. (a) TA map of RTP data. (b) TM map of RTP data. (c) TAHG map of RTP data (Black continuous lines on the map indicate the city boundaries of the study area).

4.2 Gravity data with WGM2012

In this study, the WGM2012 model was used as the gravity dataset. The WGM2012 gravity anomalies were derived from the Earth's global gravity models, EGM2008 and DTU10, and include terrain corrections with a resolution of 1′ × 1′ derived from the ETOPO1 model. These corrections consider the contribution of most surface masses, including the atmosphere, land, oceans, inland seas, lakes, ice caps, and ice shelves (Bonvalot et al., 2012). The data is available from the International Gravimetric Bureau for download at https://bgi.obs-mip.fr/data-products/gravity-databases/land-gravity-data-prod/#/data/. The use of gravity data from the WGM2012 model in the determination of geological and tectonic structures has yielded successful and important results (Eldosouky et al., 2021; Maden and Elmas, 2022). Figure 7 shows the Bouguer gravity anomaly map of Central Anatolia, Turkey. The data ranges from −101 mGal to 155 mGal.

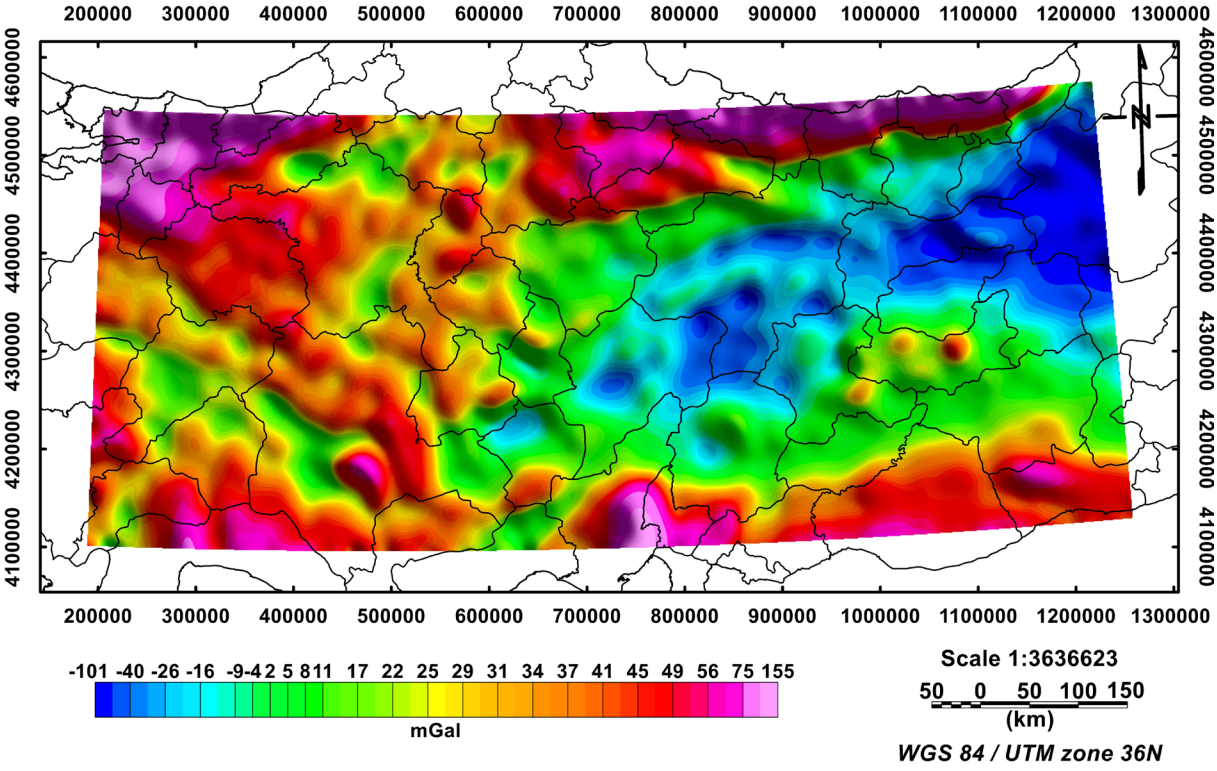

Figure 7. Bouguer gravity data (Black continuous lines on the map indicate the city boundaries of the study area).

4.2.1 Application of edge detection techniques to gravity data

The results of the THG, TA, TM, and TAHG filters applied to the data presented in Fig. 7 are shown in Fig. 8 and Figs. 9a-c, respectively. The THG (Fig. 8) filter is dominated by large-amplitude responses at the boundaries of the Central Anatolian Crystal Complex and inland areas. However, these are not balanced edge detection filters, and therefore, other detected edges are blurred, which can complicate the interpretation of the deep geological structures of the study area. The TA filter effectively compensates for anomalies at different depths but does not provide sharp signals at the boundaries (Fig. 9a). The TM map shows minimum values at source boundaries. It can be seen that the TM filter can also equalize all the different anomaly sources, but the detected edges are scattered (Fig. 9b). The maximum values in the TAHG maps provide a clear and accurate response at the structure boundaries. However, this filter could not consistently provide a clear outline of the edges of structures such as the ITSZ and IAESZ (Fig. 9c).

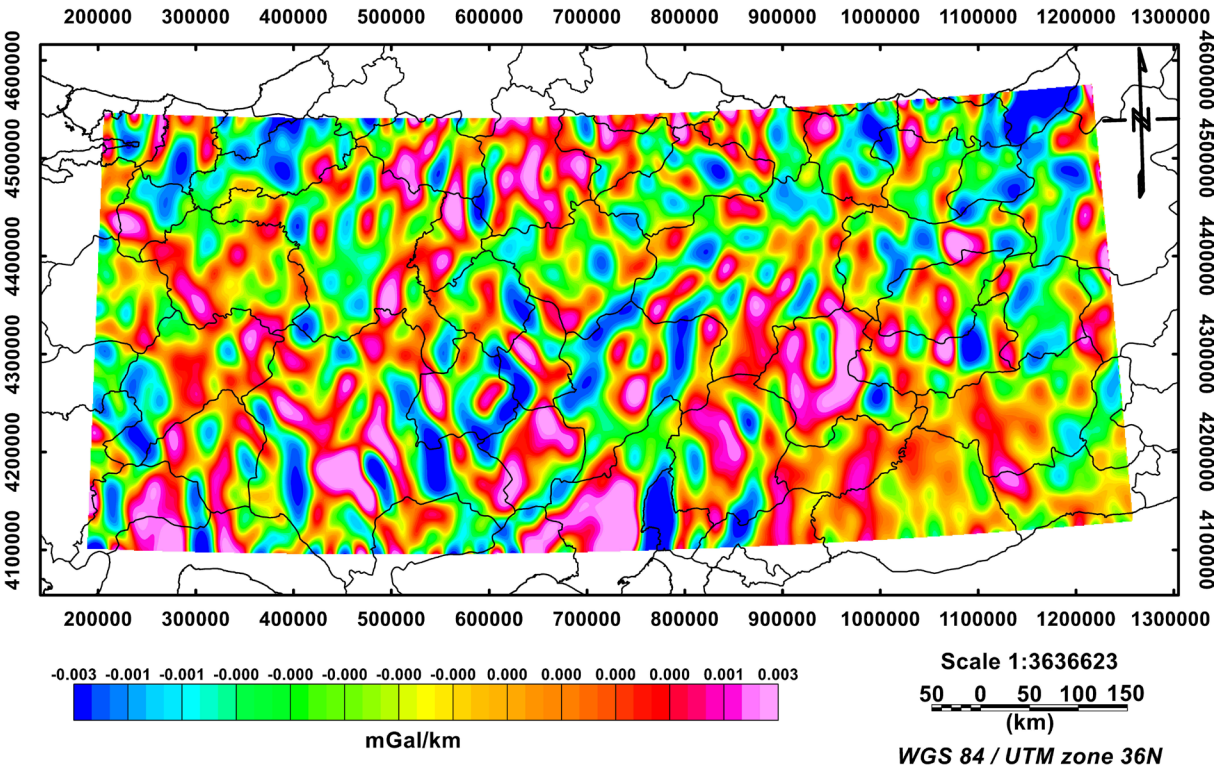

Figure 8. THG map of Bouguer gravity data (Black continuous lines on the map indicate the city boundaries of the study area).

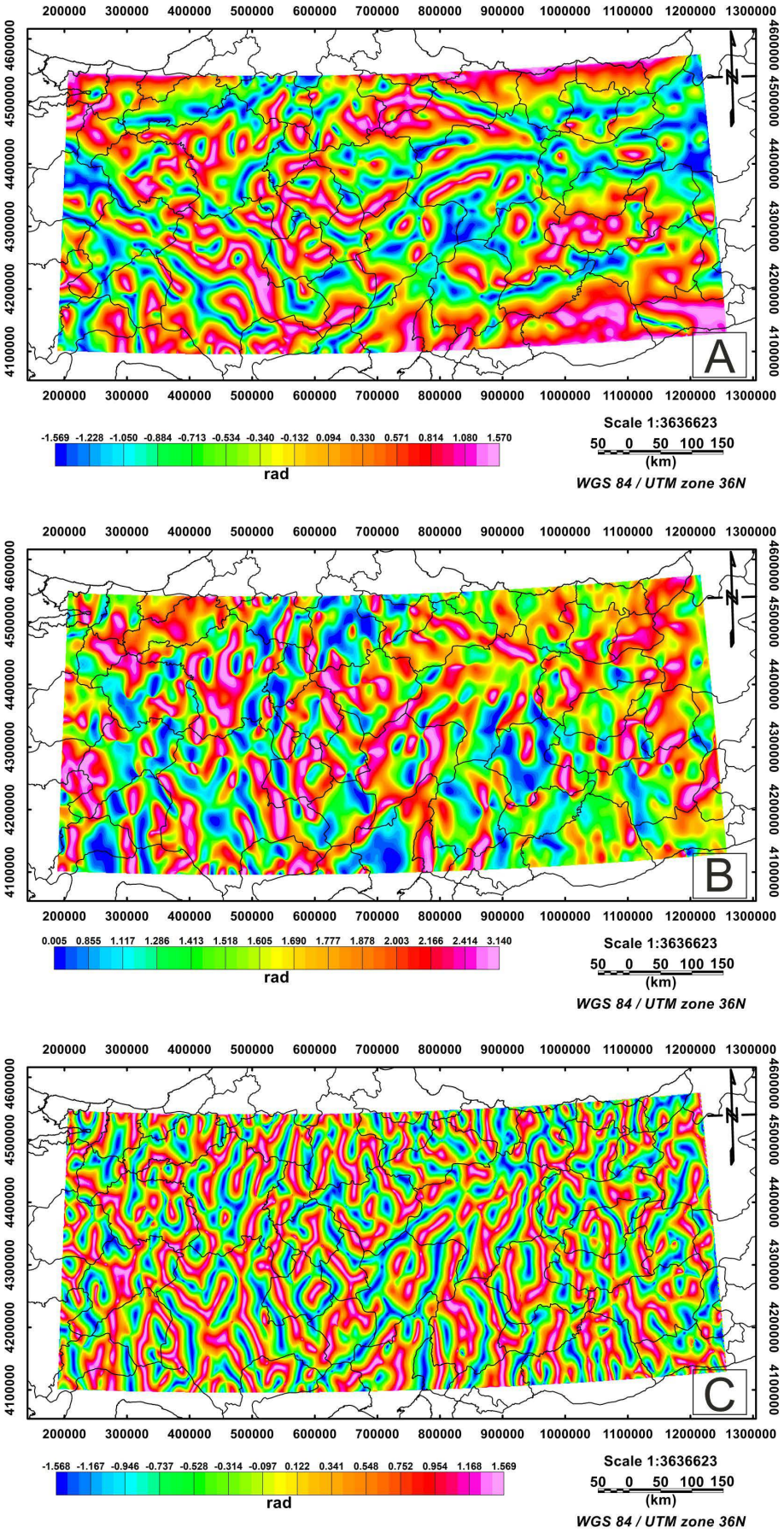

Figure 9. (a) TA map of Bouguer gravity data. (b) TM map of Bouguer gravity data. (c) TAHG map of Bouguer gravity data (Black continuous lines on the map indicate the city boundaries of the study area).

5. Discussion

The magnetic lineament map, derived from edge detection and discontinuity analyses of magnetic anomalies, reveals the location, continuity, and strike characteristics of structural elements in the study area (Fig. 10a). Figures 10a, b, and c provide complementary information regarding the structural framework of the study area. The rose diagram, prepared to evaluate the general trend and orientation distribution of lineaments, provides a statistical visualization of dominant structural trends. When the magnetic lineament map and the rose diagram, which show the strike frequencies of these lineaments, are considered together, it is seen that the main tectonic directions in the region are clearly defined and are presented in Fig. 10.

A clear and consistent structural correspondence is observed between the lineament orientations obtained from the Rose diagram and the geological and magnetic data of the study area. Three dominant directions are prominent on the diagram: NW-SE, NE-SW and E-W (Fig. 10c). These trends largely coincide with the strikes of suture zones and metamorphic-magmatic complex boundaries, which play a significant role in the tectonic evolution of Central Anatolia. The predominantly NW-SE strike of structural lineaments, particularly along the IAESZ and the ITSZ, demonstrates that the orientation distribution on the Rose diagram is consistent with the regional tectonic heritage. This same orientation also overlaps with the geometries of other important geological units, such as the Tavşanlı Zone, the Afyon Zone, and the metamorphic and granitic subunits of the Kırşehir Massif. These findings support the notion that the NW-SE trend represents a continuous deformation component throughout the geodynamic development of the region.

The distribution of magnetic anomalies also clearly reflects this structural orientation. The linear zones of high gradient observed on the anomaly map generally extend along the margins of ophiolitic units, metamorphic cores, and granitoid intrusions. This demonstrates that magnetic susceptibility differences are directly related to geological contacts and faulting geometry. In particular, the high spatial correspondence of NW-SE magnetic discontinuities with tectonic boundaries in the surface geology demonstrates that the magnetic data reliably represent the deep structural framework in the region.

The second important trend in the region, the NE-SW trend, also forms a prominent concentration on the rose diagram. This trend is known to be associated with the multidirectional deformation regime identified in the literature during the late Miocene-Quaternary tectonic evolution of Central Anatolia. The westward movement of the Anatolian block and the resulting transtensional deformation likely produced new NE-SW-trending faults and fracture zones. The partial overlap of the NE-SW-trending directions observed on the magnetic anomaly map with these young structural elements indicates that the deformation history is multi-phase and that the region bears traces of both old suture structures and new tectonic stress directions.

In this context, the high agreement between the Rose diagram, geological map, and magnetic data indicates that the lineaments in the region are not random, but rather represent a structural area shaped by the combined tectonic heritage and recent deformation. Furthermore, the systematic orientations of the magnetic anomalies indicate a strong connection between the surface geology and the deep tectonic architecture. This relationship further demonstrates the effectiveness of potential field methods, particularly in identifying fault and lithological boundaries that are not clearly visible at the surface.

In general, the obtained results indicate that the regional tectonic structure was shaped under the control of old suture zones trending NW-SE, while young NE-SW-trending deformation components reorganized the existing structural pattern.

The magnetic anomaly map shows the zone of strong high anomalies that may correspond to contacts or fractures (faults, flexures, etc.). Tectonic structural boundaries, contacts, and dip directions were determined by interpretation of data processing applied to satellite magnetic and satellite gravity data (Fig. 11). The applied edge detection analysis techniques reveal two dominant structures with NW-SE and NE-SW orientations (Fig. 10). These structural boundaries exhibiting high anomaly may correspond to ophiolitic rocks and magmatic rocks, which are generally characterized by high density anomaly values. The processing of the data reveals the presence of two main trends oriented NW-SE and NE-SW (Figs. 10, 11), which are interpreted to correspond with the main orientations of the Kırşehir Massif structures. The boundaries giving high anomalies in the magnetic anomaly maps, the geologically NW-SE extending line, coincide with the current position of the ITSZ, which is also suggested in other studies in the region (van Hinsbergen et al., 2016; Pourteau et al., 2010). Unlike the gravity map, the geologic structure boundaries are more distinct. While the granitoids belonging to the KB clearly show continuity with high amplitude magnetic anomaly values, they are clearly separated with lower value anomalies in the

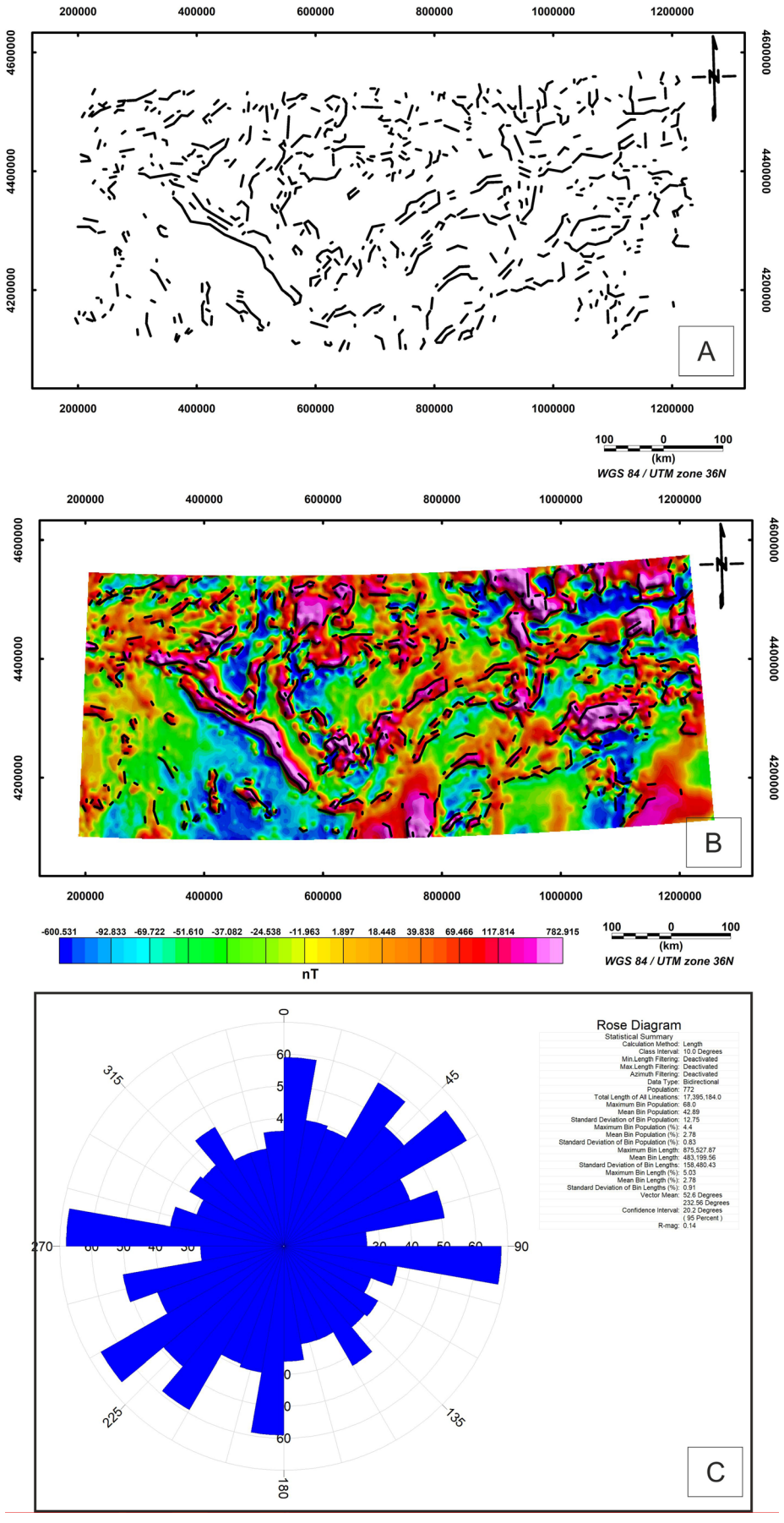

Figure 10. (a) Magnetic lineament map of the study area. (b) Superimposed map of the RTP magnetic anomaly and lineament map. (c) Rose diagram of the study area.

eastern part in the gravity data. These gravity regions, which also occasionally coincide with sedimentary basin areas, may be due to the granitoid elevations that form the KB underground (Özkaptan, 2019). When the Bouguer gravity anomaly map is examined, low gravity values are noticeable. These relatively low Bouguer gravity values are generally in the east of the study area. These areas largely coincide with the Tuz Lake Basin and the Sivas sedimentary basin.

The KB, as one of the principal tectonic domains of Anatolia, plays a critical role in understanding the geodynamic evolution of Central Anatolia. Previous studies have presented different hypotheses regarding its tectonic significance and origin. Some researchers have proposed that the KB represents an independent continental fragment, later accreted to the Sakarya Continent in the north and the Anatolide-Tauride belt in the south following the closure of the intervening Neotethyan oceanic domains (Şengör and Yılmaz, 1981; Okay and Tüysüz, 1999). The obduction of ophiolites during these collisional events left behind prominent magnetic anomalies, which are reflected in the high-intensity zones identified in this study.

The results of edge detection analyses (THG, TA, TM, and TAHG) delineate NW-SE and NE-SW trending lineaments that spatially coincide with the boundaries of the KB, particularly the IAESZ in the north and the ITSZ in the south. These findings are consistent with the tectonic model that interprets the KB as a distinct continental unit limited between these two major suture zones. The pronounced magnetic anomalies are likely associated with obducted ophiolitic sequences along these sutures, further supporting this interpretation (Parlak et al., 2009; Pourteau et al., 2010).

Similar structural correlations between geophysically derived lineaments and mapped suture zones have also been reported by Okay and Tüysüz (1999), Robertson et al. (2012), Parlak (2016), Özsöz and Toker, 2025, reinforcing the reliability of the interpreted boundaries in this study. However, Özsöz and Toker (2025) also shares the common goal of resolving the geodynamic framework of Türkiye by integrating geophysical data sets, highlighting inherited tectonic boundaries and lithospheric segmentation, and utilizing magnetic anomalies to identify structural discontinuities and crustal areas. This study, in contrast to the lithosphere-scale geodynamic synthesis presented by Özsöz and Toker (2025) for the crust-upper mantle system of Türkiye, undertakes a high-resolution, regionally focused investigation of upper-crustal magnetic lineaments, rose-diagram-derived orientation statistics, and the structural concordance between surface geology and magnetic anomaly patterns. Whereas Özsöz and Toker (2025) addressed large-scale lithospheric segmentation and mantle-crust interactions, the present work differentiates itself by elucidating the finer-scale architecture of fault geometries, the imprint of crustal tectonic inheritance, and the detailed linkages between surface structural configurations and potential-field expressions. The agreement between our geophysical results and independent geological observations indicates that the detected lineaments are not only relics of past collisional events but also zones of crustal weakness that have been reactivated under the current tectonic regime. Such reactivation processes have been documented in other segments of the IAESZ and ITSZ, highlighting their ongoing influence on regional deformation patterns.

Additionally, when compared with regional active fault maps, many of the detected lineaments exhibit a strong correlation with known active tectonic structures, suggesting that inherited crustal weaknesses along these suture zones continue to influence the present-day stress regime and neotectonic deformation in Central Anatolia. For example, the NW-SE orientation of lineaments coincides with segments of the Tuz Gölü Fault Zone and related structures, highlighting their potential significance in accommodating ongoing crustal movements.

The NW-SE and NE-SW lineaments identified in this study appear to be directly related to the crustal inheritance and deep lithospheric structure that shaped the polyphase geodynamic evolution of Central Anatolia. The NW-SE trend represents ancient zones of weakness formed by collisional tectonics that developed along the IAESZ and ITSZ during the closure of the Neotethys (Şengör and Yılmaz, 1981; Bozkurt, 2001). The observation of this trend with continuous and strong linear gradients in magnetic anomalies confirms that the deep lithological boundaries of metamorphic core complexes and granitic bodies leave a distinct signature in the magnetic field (Okay and Tüysüz, 1999). NE-SW-striking lineaments are consistent with fracture systems reactivated by the westward escape of the Anatolian block and the influence of the Aegean stress regime (McKenzie, 1972; Jackson and McKenzie, 1984).

The surface morphology also reflects this two-way deformation regime: NW-SE-trending metamorphic blocks form the elevated topography, while transtensional basins developing along NE-SW-striking faults determine the regional relief (Glover and Robertson, 1998). The relationship between this structural pattern and depth is also supported by Moho topography and crustal thickness models. The thinnest crustal thickness values occur along the Western Anatolian coasts; however, the Moho surface reaches its deepest position in Eastern Turkey

(Tezel et al., 2013). CRUST1.0, LITHO1.0, and seismic studies specific to Turkey indicate that crustal thickness reaches 36-40 km beneath the CACC and thins to 32-36 km along the ITSZ (Laske et al., 2013; Pasyanos et al., 2014; Oruç et al., 2019; Çakır et al., 2000). This crustal heterogeneity plays a decisive role in directing the discontinuities observed in magnetic anomalies.

The magnetic field is influenced by the magnetic mineral-rich upper crustal units above the Moho, rather than the Moho itself. However, the thickness and composition of the upper crust are not independent of the Moho depth. In the thick-crusted CACC region, metamorphic complexes and granitoids occupy large areas at the surface and shallow depths, producing high-amplitude and strong, persistent magnetic anomalies. In the ITSZ and other thin-crusted zones, more fractured and fragmented magnetic anomalies are observed due to the more heterogeneous and fragmented lithological distribution. Therefore, magnetic anomaly patterns are an indirect indicator of the Moho: as the Moho thickness increases, the upper crust forms more stable and massive blocks, which determine the continuity and orientation of magnetic anomaly. Regarding gravity, thicker crust (e.g., 40-45 km above the CACC-Kırşehir Massif) produces lower Bouguer gravity values because less dense continental crust forms a thicker column. Therefore, the negative gravity zones observed in the interior regions of Central Anatolia are directly related to the thickening of the crustal root. In contrast, the thinning of the crust to 30-34 km in the ITSZ and its surroundings is consistent with positive and higher gravity anomalies. Therefore, the gravity field in Central Anatolia is primarily a result of crustal thickness contrasts and density differences across suture zones.

The findings are important not only at the local level but also in a multi-scale tectonic framework. On a global scale, the lineaments in Central Anatolia provide a typical example of lithospheric reactivation observed in orogens where collision-thickening-extension processes occur sequentially (Dewey et al., 1986; Jolivet and Faccenna, 2000). At the regional scale, structural strikes form the main framework of the deformation network controlling the westward movement of Anatolia (Reilinger et al., 2006). At the local scale, magnetic and structural lineaments play a critical role in identifying fault zones, metamorphic block boundaries, and magmatic intrusions, providing directly applicable results for geological mapping.

An evaluation of magnetic (Fig. 11a) and Bouguer gravity (Fig. 11c) anomalies, combined with tilt angle transformations (Figs. 11b and 11d), reveals that the regional geological units presented in Fig. 11e exhibit distinctive signatures consistent with their physical properties. The high-amplitude, medium- to short-wavelength magnetic anomalies and positive Bouguer anomalies observed along the CACC, rich in metamorphic and granitoid components, are consistent with the high magnetic susceptibility and high-density properties of these units. The distinct and continuous gradients observed in tilt angle solutions in the same areas indicate that the basement lithologies within the CACC and the deep fracture zones bordering them can be reliably traced with geophysical data.

The metamorphic-rich ophiolitic units identified along the IAESZ and ITSZ are represented on magnetic maps by banded, high-amplitude local anomalies and associated sharp gradient zones. On the other hand, Quaternary sedimentary basins produce negative Bouguer gravity anomalies due to low magnetic amplitude and low density, which are observed as weak gradient areas on tilt angle maps. These geophysical features reflect the behavior expected from sedimentary fills with low density and weak magnetic susceptibility. The pronounced negative zone in the Tuz Lake Basin is particularly striking in the gravity anomalies. Furthermore, Fig. 11d, which shows the tilt angle map of the gravity anomalies, shows high gravity gradients along the sedimentary basin-basement rock boundaries, reflecting fault-controlled basin geometry.

In areas where Cenozoic volcanic rocks are concentrated, limited positive elevations in magnetic anomalies and sharp but narrow structural boundaries in tilt angle results are observed. This is consistent with the high magnetic mineral content of the volcanic rocks. The holistic analysis of all maps shows that there is a clear geophysical separation between the metamorphic-granitoid basement, ophiolitic units, volcanic complexes and sedimentary basins; moreover, structural boundaries within the complex neotectonic framework of the region can be reliably traced by potential field methods.

Overall, the study contributes significantly to the understanding of the multilayered tectonic architecture of Central Anatolia by holistically revealing the interaction between surface geology, magnetic anomalies, and deep crustal structure.

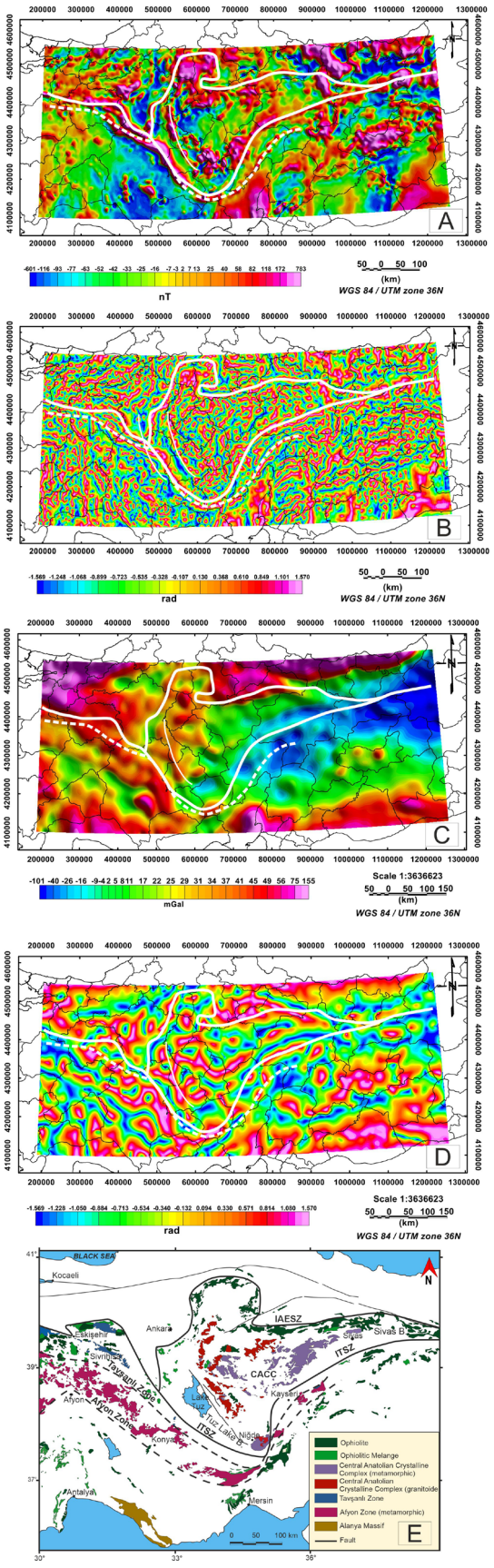

Figure 11. Structural lineaments derived from RTP magnetic anomaly and Bouguer gravity data show tectonic boundaries in the study area. (a) Tectonic lineaments on the RTP magnetic anomaly. (b) TA magnetic anomaly tectonic lineaments. (c) Bouguer gravity data tectonic lineaments. (d) TA gravity tectonic lineaments (Black continuous lines on the map indicate the city boundaries of the study area). (e) Geological map of the study area.

6. Conclusions

This study provides a detailed structural and geodynamic interpretation of the KB within the CACC by integrating global magnetic (EMAG2) and gravity (WGM2012) datasets. Boundary analyses of gravity and magnetic data were used to visualize and characterize structural boundaries and tectonic structures in the Kırşehir Massif in Central Anatolia. Using advanced edge detection techniques, we successfully identified NW-SE and NE-SW orientations tectonic lineaments, which are spatially associated with the IAESZ and the ITSZ. These findings support the hypothesis that the KB represents an independent continental fragment tectonically bounded between the Sakarya Continent to the north and the Anatolide-Tauride Platform to the south, incorporated into Anatolia during the closure of Neotethyan oceanic domains. The pronounced magnetic anomalies are interpreted as signatures of obducted ophiolites emplaced during collisional tectonics, providing additional insights into the crustal architecture beneath Central Anatolia. Furthermore, the correlation between the detected lineaments and known active fault zones suggests that inherited structural weaknesses along suture zones continue to influence the present-day stress field and neotectonic deformation of the region. These results not only refine the structural framework of Central Anatolia but also provide a robust geophysical basis for future geodynamic modeling studies aiming to reconstruct the tectonic evolution of the Kırşehir Massif and its surrounding suture zones. Overall, the integration of magnetic and gravity data presented here offers a robust approach to delineating concealed tectonic structures, complements geological mapping, and contributes to resolving long-standing debates regarding the boundaries and geodynamic evolution of the Kırşehir Massif. These results provide a useful framework for future geophysical and geological investigations aimed at unraveling the complex tectonic history of Central Anatolia.

Data availability. The EMAG2 data used in this work were obtained free of charge from the NOAA (National Oceanic and Atmospheric Administration) database. The gravity data is available from the International Gravimetric Bureau for download at https://bgi.obs-mip.fr/data-products/gravity-databases/land-gravity-data-prod/#/data/.

Acknowledgments. The author would like to thank BGI as the provider of the WGM 2012 gravity data that were used for the research, as well as the NOAA, which provided the latest EMAG2 magnetic data. I would also like to thank Z. Mümtaz Hisarlı for his valuable comments. I would also like to thank Simona Pierdominici for her constructive oversight throughout the review process. Furthermore, I thank the reviewers for their valuable comments and suggestions, which greatly improved the quality and clarity of the article.

References

Balmino, G., N. Vales, S. Bonvalot and A. Briais (2012). Spherical harmonic modelling to ultra-high degree of Bouguer and isostatic anomalies, J. Geodesy, 86, 7, 499-520, doi:10.1007/s00190-011-0533-4.

Baranov, V. (1957). A new method for interpretation of aeromagnetic maps: Pseudo-gravimetric anomalies, Geophysics, 22, 359-383, doi:10.1190/1.1438369.

Baranov, V. and H. Naudy (1964). Numerical calculation of the formula of reduction to the magnetic pole, Geophysics, 29, 1, 67-79, doi:10.1190/1.1439334.

Blakely, R. J. (1995). Potential Theory in Gravity and Magnetic Applications, Cambridge University Press, doi:10.1017/CBO9780511549816.

Bodinier, J. L. and M. Godard (2005). Orogenic, Ophiolitic, and Abyssal, The Mantle and Core, Treatise Geochem., 2, 2, 103, doi:10.1016/B0-08-043751-6/02004-1.

Bonvalot, S., G. Balmino, A. M. Briais, P. A. Kuhn et al. (2012). World gravity map, 1: 50000000 map, BGI-CGMW-CNES-IRD.

Bozkurt, E. (2001). Neotectonics of Turkey – a synthesis, Geodin. Acta, 14, 1-3, 3-30, doi:10.1080/09853111.2001.11432432.

Coleman, R. G. O. (1977). Ancient Oceanic Lithosphere? Minerals and Rocks, Springer, Berlin/Heidelberg, Germany, 12, ISBN:978-3-642-66675-9.

Cordell, L. and V. J. S. Grauch (1985). Mapping basement magnetization zones from aeromagnetic data in the San Juan Basin, New Mexico, in The Utility of Regional Gravity and Magnetic Maps, Society of Exploration Geophysicists, 181-197, doi:10.1190/1.0931830346.ch16.

Çakır, Ö., M. Erduran, H. Çınar and A. Yılmaztürk (2000). Forward modelling receiver functions for crustal structure beneath station TBZ (Trabzon, Turkey), Geophys. J. Int., 140, 2, 341-356, doi:10.1046/j.1365-246x.2000.00023.x.

Çörtük, R. M., Ö. F. Çelik, M. Özkan, J. H. Davies et al. (2024). Timing of the subduction initiation and ophiolite emplacement of the inner Tauride Ocean: Insight from the Pınarbaşı ophiolite in Central Türkiye, Lithos, 488, 107833, doi:10.1016/j.lithos.2024.107833.

Dewey, J. F., M. R. Hempton, W. S. F. Kidd, F. Saroglu et al. (1986). Shortening of continental lithosphere: the neotectonics of Eastern Anatolia – a young collision zone, Geol. Soc. London Spec. Pub., 19, 1, 1-36, doi:10.1144/GSL.SP.1986.019.01.01.

Eldosouky, A. M., L. T. Pham, R. A. El-Qassas, Z. Hamimi et al. (2021). Lithospheric structure of the Arabian-Nubian shield using satellite potential field data, The geology of the Arabian-Nubian shield, 139-151, doi:10.1007/978-3-030-72995-0_6.

Emre, Ö., T. Y. Duman, S. Özalp, H. Elmacı et al. (2013). Active Fault Map of Turkey with and Explanatory Text, General Directorate of Mineral Research and Exploration, Spec. Pub. Series, 30, Ankara, Turkey.

Ferreira, F. J. F., J. de Souza and A. B. S. Bongiolo (2013). Enhancement of the total horizontal gradient of magnetic anomalies using the tilt angle, Geophysics, 78, 3, J33-J41, doi:10.1190/geo2011-0441.1.

Glover, C. and A. Robertson (1998). Neotectonic intersection of the Aegean and Cyprus tectonic arcs: extensional and strike-slip faulting in the Isparta Angle, SW Turkey, Tectonophysics, 298, 1-3, 103-132, doi:10.1016/s0040-1951(98)00180-2.

Göncüoğlu, M. C., V. Toprak, I. Kuşcu, A. Erler et al. (1991). Geology of the western part of the Central Anatolian Massif, part 1, southern section, Turkish Petroleum Corporation, TPAO, Report 2909, 1-140, in Turkish.

Göncüoğlu, M. C., A. Erler, V. Toprak, E. Olgun et al. (1993). Geology of central part of the Central Anatolian massif: part III geological evolution of the Tertiary Basin of the Kızılırmak, Turkish Petroleum Corporation, TPAO, Report 3313, in Turkish.

Görür, N., F. Y. Oktay, I. Seymen and A. M. C. Şengör (1984). Palaeotectonic evolution of the Tuzgölü basin complex, Central Turkey: sedimentary record of a Neo-Tethyan closure, Geol. Soc. Lond. Spec. Publ., 17, 1, 467-482, doi:10.1144/GSL.SP.1984.017.01.34.

Hemant, K. and S. Maus (2005). Geological modeling of the new CHAMP magnetic anomaly maps using a geographical information system technique, J. Geophys. Res., Solid Earth, 110, B12, doi:10.1029/2005JB003837.

Hinze, W. J., R. Von Frese and A. H. Saad (2013). Gravity and magnetic exploration: Principles, practices, and applications, Cambridge University Press, ISBN:978-0-521-87101-3.

Jackson, J. and D. McKenzie (1984). Active tectonics of the Alpine – Himalayan Belt between western Turkey and Pakistan, Geophys. J. Int., 77, 1, 185-264, doi:10.1111/j.1365-246X.1984.tb01931.x.

Jolivet, L. and C. Faccenna (2000). Mediterranean extension and the Africa-Eurasia collision, Tectonics, 19, 6, 1095-1106, doi:10.1029/2000TC900018.

Ketin, İ. (1966). Anadolu'nun tektonik birlikler, Bull. Min. Res. Exp., 66, 20-34.

Laske, G., G. Masters, Z. Ma and M. Pasyanos (2013). Update on CRUST1. 0 – A 1-degree global model of Earth's crust, in Geophys. Res. Abstracts, 15, 15, 2658.

Lefebvre, C. J. C. (2011). The tectonics of the Central Anatolian Crystalline Complex: a structural, metamorphic and paleomagnetic study, Departement Aardwetenschappen.

Maden, N. and A. Elmas (2022). Major tectonic features and geodynamic setting of the Black Sea Basin: Evidence from satellite-derived gravity, heat flow, and seismological data, Tectonophysics, 824, 229207, doi:10.1016/j.tecto.2022.229207.

Maus, S., U. Barckhausen, H. Berkenbosch, N. Bournas et al. (2009). EMAG2: A 2-arc min resolution Earth Magnetic Anomaly Grid compiled from satellite, airborne, and marine magnetic measurements, Geochem. Geophys. Geosyst., 10, 8, doi:10.1029/2009GC002471.

McKenzie, D. (1972). Active tectonics of the Mediterranean region, Geophys. J. Int., 30, 2, 109-185.

Meyer, B., A. Chulliat and R. Saltus (2017). Derivation and error analysis of the Earth Magnetic Anomaly Grid at 2 arc min Resolution Version 3, EMAG2v3, Geochem. Geophys. Geosyst., 18, 12, 4522-4537, doi:10.1002/2017gc007280.

Miller, H. G. and V. Singh (1994). Potential field tilt-a new concept for location of potential field sources, J. Appl. Geophys., 32, 213-217, doi:10.1016/0926-9851(94)90022-1.

MTA, General Directorate of Mineral Research and Exploration (2002). Geological map of Turkey: General Directorate of Mineral Research and Exploration Publication, scale 1/500,000, 18 Sheets, 1:500.000, Ölçekli Türkiye Jeoloji Haritası.

Nabighian, M. N., V. J. S. Grauch, R. O. Hansen, T. R. LaFehr et al. (2005). The historical development of the magnetic method in exploration, Geophysics, 70, 6, 33ND-61ND, doi:10.1190/1.2133784.

Okay, A. I. (1984). Distribution and Characteristics of the North-west Turkish Blueschists, Geol. Soc. Spec. Publ., 17, 455-466, doi:10.1144/GSL.SP.1984.017.01.33.

Okay, A. I. (1989). Tectonic units and sutures in the Pontides, Northern Turkey, in Tectonic evolution of the Tethyan region A. M. C. Şengör (Ed.), Kluwer Academic Publication, 109-116, doi:10.1007/978-94-009-2253-2_6.

Okay, A. I. and O. Tüysüz (1999). Tethyan sutures of northern Turkey, Geol. Soc. Lond. Spec. Publ., 156, 1, 475-515, doi:10.1144/GSL.SP.1999.156.01.22.

Okay, A. I., A. M. C. Şengör and N. Görür (1994). Kinematic history of the opening of the Black Sea and its effect on the surrounding regions, Geology, 22, 267-270, doi:10.1130/0091-7613(1994)022<0267:KHOTOO>2.3.CO;2.

Oruç, B., O. Pamukcu and T. Sayın (2019). Isostatic Moho undulations and estimated elastic thicknesses of the lithosphere in the central Anatolian plateau, Turkey, J. Asian Earth Sci., 170, 166-173, doi:10.1016/j.jseaes.2018.11.001.

Özkaptan, M. (2019). Orta Anadolu (Ankara ve civarı) Havzalarının Gravite & Manyetik Yöntemler ile Modellenmesi, Türkiye Jeoloji Bülteni, 62, 2, 141-166, doi:10.25288/tjb.546581.

Özsöz, İ. and C. E. Toker (2025). From back-arc extension to continental collision: A geophysical view of the Anatolian lithosphere, Tectonophysics, 230929, doi:10.1016/j.tecto.2025.230929.

Pasyanos, M. E., T. G. Masters, G. Laske and Z. Ma (2014). LITHO1. 0: An updated crust and lithospheric model of the Earth, J. Geophys. Res., Solid Earth, 119, 3, 2153-2173, doi:10.1002/2013JB010626.

Parlak, O. (2016). The tauride ophiolites of Anatolia (Turkey): A review, J. Earth Sci., 27, 6, 901-934, doi:10.1007/s12583-016-0679-3.

Parlak, O., T. Rızaoğlu, U. Bağcı, F. Karaoğlan et al. (2009). Tectonic significance of the geochemistry and petrology of ophiolites in southeast Anatolia, Turkey, Tectonophysics, 473, 1-2, 173-187, doi:10.1016/j.tecto.2008.08.002.

Pham, L. T., E. Oksum, T. D. Do and M. L. Huy (2018). New method for edges detection of magnetic sources using logistic function, Geofizicheskiy Zhurnal, 40, 127-135, doi:10.24028/gzh.0203-3100.v40i6.2018.151033.

Pham, L. T., T. Van Vu, S. Le Thi and P. T. Trinh (2020). Enhancement of potential field source boundaries using an improved logistic filter, Pure Appl. Geophys., 177, 5237-5249, doi:10.1007/s00024-020-02542-9.

Pourteau, A., O. Candan and R. Oberhänsli (2010). High-pressure metasediments in central Turkey: Constraints on the neotethyan closure history, Tectonics, 29, TC5004, doi:10.1029/2009TC002650.

Reilinger, R., S. McClusky, P. Vernant, S. Lawrence et al. (2006). GPS constraints on continental deformation in the Africa-Arabia-Eurasia continental collision zone and implications for the dynamics of plate interactions, J. Geophys. Res., Solid Earth, 111, B5, doi:10.1029/2005JB004051.

Robertson, A. H. F., O. Parlak and T. Ustaömer (2012). Overview of the Palaeozoic-Neogene evolution of Neotethys in the Eastern Mediterranean region (Southern Turkey, Cyprus, Syria), Pet. Geosci., 18, 4, 381-404, doi:10.1144/petgeo2011-091.

Robertson, A. H. F., O. Parlak and T. Ustaömer (2013). Late Palaeozoic-Early Cenozoic tectonic development of Southern Turkey and the easternmost Mediterranean region: Evidence from the inter-relations of continental and oceanic units, Geol. Soc. Lond. Spec. Publ., 372, 9-48, doi:10.1144/SP372.22.

Salem, A., S. Williams, D. Fairhead, R. Smith et al. (2008). Interpretation of magnetic data using tilt-angle derivatives, Geophysics, 73, 1, L1-L10, doi:10.1190/1.2799992.

Şaroğlu, F., O. Emre and I. Kuşcu (1992). Active fault map of Turkey, General Directorate of Mineral Research and Exploration, Ankara, Turkey.

Şengör, A. M. C. and Y. Yılmaz (1981). Tethyan evolution of Turkey: a plate tectonic approach, Tectonophysics, 75, 3-4, 181-241.

Taymaz, T., Y. Yılmaz and Y. Dilek (2007). The geodynamics of the Aegean and Anatolia: introduction, Geol. Soc. Lond. Spec. Publ., 291, 1, 1-16, doi:10.1144/SP291.1.

Temiz, U., E. Gökten and J. Eikenberg (2009). U/Th dating of fissure ridge travertines from the Kirsehir region (Central Anatolia Turkey): structural relations and implications for the Neotectonic development of the Anatolian block, Geodin. Acta, 22, 4, 201-213, doi:10.3166/ga.22.201-213.

Tezel, T., T. Shibutani and B. Kaypak (2013). Crustal thickness of Turkey determined by receiver function, J. Asian Earth Sci., 75, 36-45, doi:10.1016/j.jseaes.2013.06.016.

van Hinsbergen, D. J., M. Maffione, A. Plunder, N. Kaymakcı et al. (2016). Tectonic evolution and paleogeography of the Kırşehir Block and the Central Anatolian Ophiolites, Turkey, Tectonics, 35, 4, 983-1014, doi:10.1002/2015TC004018.

Verduzc, B., J. D. Fairhead, C. M. Green and C. MacKenzie (2004) New insights into magnetic derivatives for structural mapping, Lead Edge, 23, 2, 116-119, doi:10.1190/1.1651454.

Wessel, P., W. H. F. Smith, R. Scharroo, J. Luis et al. (2013). Generic Mapping Tools: Improved version released, EOS Trans., AGU, 94, 45, 409-410, doi:10.1002/2013EO450001.

Whitney, D. L. and Y. Dilek (1998). Metamorphism during Alpine crustal thickening and extension in Central Anatolia, Turkey: The Niğde metamorphic core complex, J. Petrol., 39, 7, 1385-1403.

Wijns, C., C. Perez and P. Kowalczyk (2005). Theta map: Edge detection in magnetic data, Geophysics, 70, 4, L39-43, doi:10.1190/1.1988184.

Yılmaz, Y., E. Yiğitbaş and Ş. C. Genç (1993). Ophiolitic and metamorphic assemblages of southeast Anatolia and their significance in the geological evolution of the orogenic belt, Tectonics, 12, 5, 1280-1297, doi:10.1029/93TC00597.

Yılmaz, Y., Ş. C. Genç, E. Yiğitbaş, M. Bozcu et al. (1995). Geological evolution of the late Mesozoic continental margin of Northwestern Anatolia, Tectonophysics, 243, 1-2, 155-171, doi:10.1016/0040-1951(94)00196-G.

Yılmaz, Y., H. S. Serdar, C. Genç, E. Yigitbas et al. (1997). The geology and evolution of the Tokat Massif, south-central Pontides, Turkey, Int. Geol. Rev., 39, 4, 365-382, doi:10.1080/00206819709465278.

***CORRESPONDING AUTHOR: Gulten AKTAS**,
Gümüşhane University, Department of Geophysical Engineering, Gümüşhane, Turkey
email: gultenaktas@gumushane.edu.tr